
A Scalable Evolution Strategy with Directional Gaussian Smoothing for Blackbox Optimization

Jiaxin Zhang^{1*} Hoang Tran^{1*} Dan Lu^{2*} Guannan Zhang^{1*}

Abstract

We developed a new scalable evolution strategy with directional Gaussian smoothing (DGS-ES) for high-dimensional blackbox optimization. Standard ES methods have been proved to suffer from the curse of dimensionality, due to the random directional search and low accuracy of Monte Carlo estimation. The key idea of this work is to develop Gaussian smoothing approach which only averages the original objective function along d orthogonal directions. In this way, the partial derivatives of the smoothed function along those directions can be represented by one-dimensional integrals, instead of d -dimensional integrals in the standard ES methods. As such, the averaged partial derivatives can be approximated using the Gauss-Hermite quadrature rule, as opposed to MC, which significantly improves the accuracy of the averaged gradients. Moreover, the smoothing technique reduces the barrier of local minima, such that global minima become easier to achieve. We provide three sets of examples to demonstrate the performance of our method, including benchmark functions for global optimization, and a rocket shell design problem.

1. Introduction

Evolution strategy (ES) is a class of blackbox optimization algorithms often used to optimize functions when gradient information is inaccessible. Let $F(\boldsymbol{x})$ be an objective function in \mathbb{R}^d , we are interested in searching for \boldsymbol{x} with function value $F(\boldsymbol{x})$ as small as possible, where the only available information is the function values evaluated at search points. In recent years, ES has been revived as a popular method in several machine learning problems including optimiz-

ing neural networks (Cui et al., 2018) and reinforcement learning (Salimans et al., 2017; Fazel et al., 2018).

In this work, we are interested in a particular class of ES methods, which represents the population by multivariate Gaussian distributions. This type of ES can be viewed as optimizing a modified objective function with Gaussian smoothing (GS). The key step of GS-based evolution strategy, is the computation of efficient search directions (most commonly, gradient) for F based on the GS formula. In (Flaxman et al., 2005; Nesterov & Spokoiny, 2015), the authors studied a random optimization technique, where the search direction is randomly chosen and the updates are generated from an estimate of directional derivative. It was shown in (Salimans et al., 2017) that the evaluation of $F(\boldsymbol{x})$ and estimation of directional derivatives can be performed in parallel to provide a gradient estimate at each searching step. This scheme is simple and suitable for large-scale distributed optimization. There have been several attempts to improve the gradient estimate by carefully selecting the directions along which the gradient information is aggregated, for example, by using orthogonal instead of Monte-Carlo directions (Choromanski et al., 2018), exploiting the past data (Maheswaranathan et al., 2019; Meier et al., 2019), and employing active subspaces (Choromanski et al., 2019a).

One prominent challenge in blackbox optimization is that the landscape of $F(\boldsymbol{x})$ is often complex and possesses plentiful of local minima and saddle points. There is a risk for any optimization algorithm, with or without access to full gradients, to get trapped in some of those points and become stagnate. The Gaussian smoothing, with its ability to smooth out function and damps out small, insignificant fluctuations, is a strong candidate in this very task. Specifically, with a moderately large smoothing parameter (i.e., strong smoothing effect), we can expect the gradient of the smoothed objective function will be able to look outside unimportant variation in the adjacent area and detect the general trend of the function from a distance, therefore an efficient *nonlocal* search direction. This potential of GS, however, has not been a focus of current works on ES, many of which concern with improving the accuracy of local gradient estimators (Maheswaranathan et al., 2019; Meier et al., 2019; Berahas et al., 2019a; Choromanski et al., 2019b).

*Equal contribution ¹Computer Science and Mathematics Division, Oak Ridge National Laboratory, TN 37831, USA ²Computational Science and Engineering Division, Oak Ridge National Laboratory, TN 37831, USA. Correspondence to: Guannan Zhang <zhangg@ornl.gov>.

Yet, the local gradient may be misleading (see Figure 1).

Another challenge in estimating search direction arises from the high dimensionality of the objective functions. Indeed, the common approach to compute the gradient of Gaussian smoothed function is by numerical integration, for which, roughly speaking, one needs to feed with function evaluations from a domain with diameter proportional to the smoothing parameter. By increasing this parameter, we also significantly enlarge the domain, especially in high-dimensional cases, and the number of function evaluations for each gradient estimate can become prohibitively large.

In this paper, we propose an enhancement to ES by introducing a directional Gaussian smoothing (DGS)-gradient operator for determining nonlocal search direction, which takes into account large scale variation of the function and disregard local fluctuation. This DGS-gradient resembles the gradient of Gaussian smoothed version of the objective function with a moderately large smoothing parameter. As computing this gradient involves a d -dimensional numerical integration and is very costly, the key idea of the DGS-gradient is to average the original objective function along d orthogonal directions for the partial derivatives, and then, aggregates the information of all partial derivatives to assemble the full DGS-gradient. This strategy requires d one-dimensional numerical integration, instead of one d -dimensional, thus significantly reduces the number of function evaluations. We call our method *directional Gaussian smoothing ES* (DGS-ES) in the rest of the paper.

To maintain high accuracy for each partial derivative estimate, we use the Gauss-Hermite quadrature rule in each direction. While the DGS-gradient can be seen as a perturbed version of the gradient of Gaussian smoothed objective function, it is worth remarking that this operator may not form a gradient field of any function. We verify that in local regime (i.e., small smoothing parameter), the DGS-gradient operator is consistent with the local gradient. Furthermore, we proved that our method has a theoretical convergence rate independence of dimension, superior to that of GS-ES based on Monte Carlo sampling. The main contributions of this work can be summarized as follows:

- Development of the DGS-gradient operator and its Gauss-Hermite estimator, which introduces an effective nonlocal search direction generation approach into the family of Evolution Strategy.
- Theoretical analysis verifying the scalability of the DGS-ES method, i.e., the number of iteration needed for convergence is *independent* of the dimension for strongly convex functions.
- Demonstration of our DGS-ES method on both high-dimensional non-convex benchmark optimization problems, as well as a real-world material design problem for rocket shell manufacture.

1.1. Related works

ES is an instance of derivative-free optimization that employs random search techniques to optimize an objective function (Rechenberg & Eigen, 1973; Schwefel, 1977). The search can be guided via either covariance matrix adaptation (Hansen & Ostermeier, 2001; Hansen, 2016), or search gradients to be fed to first order optimization schemes, (Wierstra et al., 2014). Our work herein is in line with the second approach. Recent applications of ES can be found in reinforcement learning (Houthoofd et al., 2018; Ha & Schmidhuber, 2018), meta-learning (Metz et al., 2018), optimizing neural network architecture (Real et al., 2017; Miikkulainen et al., 2017), and direct training of neural network (Morse & Stanley, 2016). Gaussian smoothed emerged a method for approximating gradient as a search direction for ES (Flaxman et al., 2005; Nesterov & Spokoiny, 2015). This approach can be combined with trust region methods for optimization (Maggiar et al., 2018). A closely related approach is sphere smoothed (Flaxman et al., 2005). A comparison of different methods for gradient approximation, including finite difference, Gaussian smoothed and sphere smoothed, can be found in (Berahas et al., 2019b). Finally, for general review on derivative-free optimization, we refer to (Rios & Sahinidis, 2009; Larson et al., 2019)

2. Background

We are interested in solving the following blackbox optimization problem

$$\min_{\mathbf{x} \in \mathbb{R}^d} F(\mathbf{x}), \quad (1)$$

where $\mathbf{x} = (x_1, \dots, x_d) \in \mathbb{R}^d$ consists of d tuning parameters, and $F : \mathbb{R}^d \rightarrow \mathbb{R}$ is a high-dimensional blackbox objective function. In this work, we assume that the gradient $\nabla F(\mathbf{x})$ is not available, and that the function $F(\mathbf{x})$ is only accessible via function evaluations. Unless otherwise stated, we do not assume $F(\mathbf{x})$ is convex.

We briefly recall the class of ES methods, e.g., (Hansen & Ostermeier, 2001; Salimans et al., 2017), which uses the multivariate Gaussian distribution to represent the population. In other words, those ES methods were developed based on Gaussian smoothing (Flaxman et al., 2005; Nesterov & Spokoiny, 2015) of $F(\mathbf{x})$ in Eq. (1), i.e.,

$$\begin{aligned} F_{\boldsymbol{\sigma}}(\mathbf{x}) &= \frac{1}{(2\pi)^{\frac{d}{2}}} \int_{\mathbb{R}^d} F(\mathbf{x} + \boldsymbol{\sigma} \circ \mathbf{u}) e^{-\frac{1}{2}\|\mathbf{u}\|_2^2} d\mathbf{u} \quad (2) \\ &= \mathbb{E}_{\mathbf{u} \sim \mathcal{N}(0, \mathbf{I}_d)} [F(\mathbf{x} + \boldsymbol{\sigma} \circ \mathbf{u})], \end{aligned}$$

where the original objective function $F(\mathbf{x})$ is smoothed via a convolution with a d -dimensional Gaussian distribution $\mathcal{N}(0, \mathbf{I}_d)$, the notation \circ represents the element-wise product, and the vector $\boldsymbol{\sigma} = (\sigma_1, \dots, \sigma_d)$ plays the role of a smoothing parameter. In general, the smoothed function $F_{\boldsymbol{\sigma}}$

has better properties than $F(\mathbf{x})$, as all the characteristics of $F(\mathbf{x})$, e.g., convexity, the Lipschitz constant, are inherited by $F_\sigma(\mathbf{x})$. Moreover, for any $\sigma > 0$, the function F_σ is always differentiable even if F is not. As the discrepancy between the gradients of F and F_σ can be bounded by the Lipschitz constant (see (Nesterov & Spokoiny, 2015) Lemma 3 for details), the original optimization problem in Eq. (1) can be replaced by a smoothed version, i.e., $\min_{\mathbf{x} \in \mathbb{R}^d} F_\sigma(\mathbf{x})$. The gradient of $F_\sigma(\mathbf{x})$ is given by

$$\begin{aligned} \nabla F_\sigma(\mathbf{x}) &= \frac{1}{(2\pi\|\boldsymbol{\sigma}\|_2)^{\frac{d}{2}}} \int_{\mathbb{R}^d} F(\mathbf{x} + \boldsymbol{\sigma} \circ \mathbf{u}) \mathbf{u} e^{-\frac{1}{2}\|\mathbf{u}\|_2^2} d\mathbf{u}, \\ &= \frac{1}{\|\boldsymbol{\sigma}\|_2^{d/2}} \mathbb{E}_{\mathbf{u} \sim \mathcal{N}(0, \mathbf{I}_d)} [F(\mathbf{x} + \boldsymbol{\sigma} \circ \mathbf{u}) \mathbf{u}]. \end{aligned} \quad (3)$$

The standard ES method refers to the algorithm that uses Monte Carlo sampling to estimate the gradient $\nabla F_\sigma(\mathbf{x})$ and update the state \mathbf{x} from iteration t to $t+1$ by $\mathbf{x}_{t+1} = \mathbf{x}_t - \frac{\lambda}{M\sigma} \sum_{m=1}^M F(\mathbf{x} + \boldsymbol{\sigma} \circ \mathbf{u}_m)$, where λ is the learning rate, \mathbf{u}_m are sampled from the Gaussian distribution $\mathcal{N}(0, \mathbf{I}_d)$.

One major advantage of the ES methods is that they are suited to be scaled up to a large number of parallel workers. All the function evaluations within each iteration can be simulated totally in parallel, and each worker only needs to return a scalar to the master, such that the communication cost among workers is almost minimal. Even though the existing ES methods and their variants have been successful in solving blackbox optimization problem in low to medium dimensions, the performance of the existing ES methods drops significantly when the dimension increases, especially in the case of having non-convex objective functions. Thus, the motivation of this work is to advance the state of the art of the ES type methods in solving high-dimensional non-convex optimization problems.

3. The evolution strategy with directional Gaussian smoothing (DGS-ES)

We present our main contributions in this section. We start by introducing, in §3.1, a novel directional Gaussian smoothing approach, in which the objective function $F(\mathbf{x})$ is smoothed along d -orthogonal directions, as opposed to the isotropic smoothing in Eq. (2). The DGS-gradient operator will be then introduced, followed by its approximation using the Gauss-Hermite quadrature rule. In §3.2, we describe the details of the proposed DGS-ES algorithm, and its convergence analysis is then provided in §3.3.

3.1. The DGS-gradient operator

To proceed, we first define a *one-dimensional* function

$$G(y | \mathbf{x}, \boldsymbol{\xi}) = F(\mathbf{x} + y \boldsymbol{\xi}), \quad y \in \mathbb{R}, \quad (4)$$

where \mathbf{x} is the current state of the objective function $F(\mathbf{x})$ and $\boldsymbol{\xi}$ is a unit vector in \mathbb{R}^d . Note that \mathbf{x} and $\boldsymbol{\xi}$ can be viewed as parameters of the function G . We define the Gaussian smoothing of $G(y)$, denoted by $G_\sigma(y)$, by

$$\begin{aligned} G_\sigma(y | \mathbf{x}, \boldsymbol{\xi}) &:= \frac{1}{\sqrt{2\pi}} \int_{\mathbb{R}} G(y + \sigma v | \mathbf{x}, \boldsymbol{\xi}) e^{-\frac{v^2}{2}} dv \\ &= \mathbb{E}_{v \sim \mathcal{N}(0,1)} [G(y + \sigma v | \mathbf{x}, \boldsymbol{\xi})], \end{aligned} \quad (5)$$

which is the Gaussian smoothing of $F(\mathbf{x})$ along the direction $\boldsymbol{\xi}$ in the neighbourhood of \mathbf{x} . It is easy to see that the derivative of $G_\sigma(y | \mathbf{x}, \boldsymbol{\xi})$ at $y = 0$ is represented by

$$\begin{aligned} \mathcal{D}[G_\sigma(0 | \mathbf{x}, \boldsymbol{\xi})] &= \frac{1}{\sqrt{2\pi}\sigma} \int_{\mathbb{R}} G(\sigma v | \mathbf{x}, \boldsymbol{\xi}) v e^{-\frac{v^2}{2}} dv, \\ &= \frac{1}{\sigma} \mathbb{E}_{v \sim \mathcal{N}(0,1)} [G(\sigma v | \mathbf{x}, \boldsymbol{\xi}) v], \end{aligned} \quad (6)$$

where \mathcal{D} denotes the differential operator. As opposed to directional derivatives of $F_\sigma(\mathbf{x})$, the derivative $\mathcal{D}[G_\sigma(0 | \mathbf{x}, \boldsymbol{\xi})]$ only involves the directionally smoothed objective function given in Eq. (5).

Now it is natural to define a DGS-gradient operator for $F(\mathbf{x})$ by building directional derivatives in Eq. (6) for d orthogonal directions, i.e.,

$$\nabla_{\boldsymbol{\sigma}, \boldsymbol{\Xi}}[F](\mathbf{x}) = \boldsymbol{\Xi}^\top \begin{bmatrix} \mathcal{D}[G_{\sigma_1}(0 | \mathbf{x}, \boldsymbol{\xi}_1)] \\ \vdots \\ \mathcal{D}[G_{\sigma_d}(0 | \mathbf{x}, \boldsymbol{\xi}_d)] \end{bmatrix}, \quad (7)$$

where $\boldsymbol{\Xi} := (\boldsymbol{\xi}_1, \dots, \boldsymbol{\xi}_d)^\top$ represents the matrix consisting of d orthonormal vectors. It is important to notice that the DGS-gradient in Eq. (7) is not equal to $\nabla F_\sigma(\mathbf{x})$ for a general smoothing factor σ , because of the directional Gaussian smoothing used in Eq. (7). However, there is consistency between the two quantities as $\sigma \rightarrow 0$, i.e.,

$$\lim_{\sigma \rightarrow 0} |\nabla F_\sigma(\mathbf{x}) - \nabla_{\boldsymbol{\sigma}, \boldsymbol{\Xi}}[F](\mathbf{x})| = 0, \quad (8)$$

for fixed \mathbf{x} and $\boldsymbol{\Xi}$. In particular, if $\nabla F(\mathbf{x})$ exists, both quantities will converge to $\nabla F(\mathbf{x})$ as $\sigma \rightarrow 0$. Such consistency naturally led to the idea of replacing $\nabla F_\sigma(\mathbf{x})$ with $\nabla_{\boldsymbol{\sigma}, \boldsymbol{\Xi}}[F](\mathbf{x})$ in the ES framework.

3.2. The DGS-ES algorithm

The key idea of the DGS-ES algorithm is to exploit the fact that each component of $\nabla_{\boldsymbol{\sigma}, \boldsymbol{\Xi}}[F](\mathbf{x})$ in Eq. (7) only involves a one-dimensional integral, such that Gauss quadrature rules (Quarteroni et al., 2007) can be used to approximate the integrals with *spectral* convergence. In this work, we utilize the Gauss-Hermite (GH) quadrature rule, which was designed for computing integrals of the form $\int_{\mathbb{R}} g(x) e^{-x^2} dx$. By doing a simple change of variable in Eq. (6), the GH rule

can be directly used to obtain the following approximation formula for $\mathcal{D}[G_\sigma(0 | \mathbf{x}, \boldsymbol{\xi})]$, i.e.,

$$\begin{aligned} & \tilde{\mathcal{D}}^M[G_\sigma(0 | \mathbf{x}, \boldsymbol{\xi})] \\ & := \frac{1}{\sqrt{\pi}\sigma} \sum_{m=1}^M w_m G(\sqrt{2}\sigma v_m | \mathbf{x}, \boldsymbol{\xi}) \sqrt{2}v_m \\ & = \frac{1}{\sqrt{\pi}\sigma} \sum_{m=1}^M w_m F(\mathbf{x} + \sqrt{2}\sigma v_m \boldsymbol{\xi}) \sqrt{2}v_m \end{aligned} \quad (9)$$

where w_m , $m = 1, \dots, M$ are the GH quadrature weights defined by $w_m = \frac{2^{M+1}M!\sqrt{\pi}}{[H'_M(v_m)]^2}$, v_m , $m = 1, \dots, M$, are the roots of the Hermite polynomial of degree M $H_M(v) = (-1)^M e^{v^2} \frac{d^M}{dv^M}(e^{-v^2})$, and M is the number of function evaluations needed to compute the quadrature in Eq. (9). The weights $\{w_m\}_{m=1}^M$ and the roots $\{v_m\}_{m=1}^M$ can be found in (Abramowitz & Stegun, 1972). The approximation error of the GH formula can be bounded by $\tilde{\mathcal{D}}^M[G_\sigma]$ is

$$\left| \tilde{\mathcal{D}}^M[G_\sigma] - \mathcal{D}[G_\sigma] \right| \leq C_0 \frac{M! \sqrt{\pi}}{2^M (2M)!} \sigma^{2M-1}, \quad (10)$$

where $M!$ is the factorial of M , and the constant $C_0 > 0$ is independent of M and σ .

Applying the GH quadrature rule $\tilde{\mathcal{D}}^M$ to each component of $\nabla_{\sigma, \Xi}[F](\mathbf{x})$ in Eq. (7), we define the following estimator:

$$\tilde{\nabla}_{\sigma, \Xi}^M[F](\mathbf{x}) := \Xi^\top \begin{bmatrix} \tilde{\mathcal{D}}^M[G_{\sigma_1}(0 | \mathbf{x}, \boldsymbol{\xi}_1)] \\ \vdots \\ \tilde{\mathcal{D}}^M[G_{\sigma_d}(0 | \mathbf{x}, \boldsymbol{\xi}_d)] \end{bmatrix}, \quad (11)$$

which requires a total of $M \times d$ *parallelizable* function evaluations. In the DGS-ES algorithm, we use $\tilde{\nabla}_{\sigma, \Xi}^M[F](\mathbf{x})$, instead of the estimators of $\nabla F_\sigma(\mathbf{x})$ in the literature, to update \mathbf{x} . For example, a simple update of \mathbf{x} would be

$$\mathbf{x}_{t+1} = \mathbf{x}_t - \lambda \tilde{\nabla}_{\sigma, \Xi}^M[F](\mathbf{x}_t). \quad (12)$$

According to the consistency result in Eq. (8), the update \mathbf{x}_{t+1} will converge to the standard ES update using ∇F_σ as $\sigma \rightarrow 0$, which is also the gradient descent update if ∇F exists. As such, the DGS-ES method is expected to have comparable performance as the standard ES or gradient descent methods for small values of σ .

On the other hand, the spectral convergence of the GH quadrature guarantees that $\tilde{\nabla}_{\sigma, \Xi}^M[F](\mathbf{x})$ is an accurate estimator of the DGS-gradient for a small M , regardless of the value of σ . This fact enables the use of relatively big values of σ in Eq. (11) to exploit the *nonlocal* features of $F(\mathbf{x})$ in the optimization process. The nonlocal exploitation ability of $\tilde{\nabla}_{\sigma, \Xi}^M[F]$ is demonstrated in §4 to be effective in skipping local minima of the objective function $F(\mathbf{x})$. An illustration of the nonlocal exploitation is given in Figure 1.

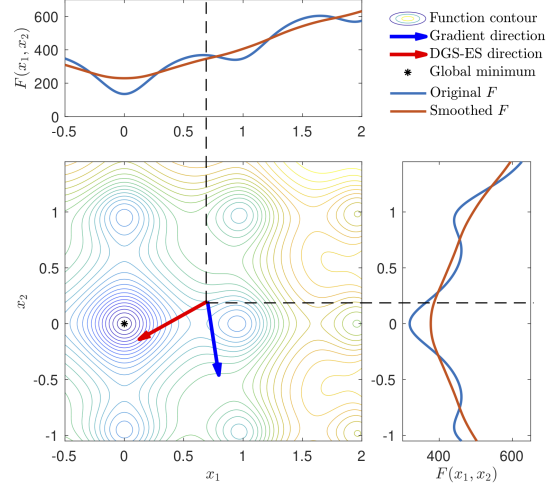


Figure 1. Illustration of the nonlocal exploitation ability of the DGS smoothing technique. The blue arrow points to the *local* gradient direction, and the red arrow points to the DGS-gradient direction, where the directionally smoothed functions along the two axes are the red curves in the top and right sub-figures. As the DGS smoothing captures the nonlocal features of $F(x_1, x_2)$, the DGS-gradient points to a much better direction, i.e., closer to the global minimum, than the local gradient.

Random perturbation of Ξ and σ for exploration. As the GH weights w_m and v_m , $m = 1, \dots, M$, are deterministic values, the estimator $\tilde{\nabla}_{\sigma, \Xi}^M[F](\mathbf{x})$ in Eq. (11) is a *deterministic* estimator for fixed Ξ and σ . This means the entire optimization algorithm will be deterministic if Eq. (12) is used to update \mathbf{x} . Compared to the standard ES and its variants, there is a lack of random exploration in our approach. The optimizer may be trapped in a local minimum without a random exploration strategy when minimizing a non-convex function. To alleviate this issue, we add random perturbation to Ξ and σ . For the orthonormal matrix Ξ , we intend to add a small random perturbation, denoted by $\Delta\Xi$, such that the orthonormal system defined by $\Xi_{\text{new}} = \Xi + \Delta\Xi$ is a small random rotation from Ξ . Since $\Delta\Xi_{\text{new}}$ needs to be orthonormal, we have

$$\begin{aligned} \mathbf{I}_d &= \Xi_{\text{new}}^\top \Xi_{\text{new}} = (\Xi + \Delta\Xi)^\top (\Xi + \Delta\Xi) \\ &= \mathbf{I}_d + \Xi^\top \Delta\Xi + \Delta\Xi^\top \Xi + \Delta\Xi^\top \Delta\Xi. \end{aligned}$$

By neglecting the high-order term $\Delta\Xi^\top \Delta\Xi$, we conclude that the infinitesimal rotation matrix $\Delta\Xi$ is a skew-symmetric matrix, i.e., $\Delta\Xi^\top = -\Delta\Xi$. In practice, we construct Ξ_{new} by creating a random skew-symmetric matrix with small-value entries, adding it to the current Ξ , and pushing it through the Gram-Schmidt process for orthonormalization. We denote by $\alpha > 0$ the multiplier that is used to control the magnitude of the entries of $\Delta\Xi$.

The perturbation of σ is conducted by drawing random samples from a uniform distribution $U(r-\beta, r+\beta)$ with two hyper-parameters r and β with $r - \beta > 0$. The frequency

of random perturbation can be determined by various types of indicators, e.g., the magnitude of the DGS-gradient, the number of iteration done since last perturbation.

Algorithm 1: The DGS-ES algorithm

1: Hyper-parameters:

M : the order of GH quadrature rule

λ : learning rate

α : the scaling factor for controlling the norm of $\Delta\Xi$

r, β : the mean and radius for sampling σ

γ : the tolerance for triggering random perturbation

2: Input: The initial state \mathbf{x}_0
3: Output: The final state \mathbf{x}_T

4: Set $\Xi = \mathbf{I}_d$, and $\sigma_i = r$ for $i = 1, \dots, d$

5: **for** $t = 0, \dots, T - 1$ **do**

6: Evaluate $\{G(\sqrt{2}\sigma_i v_m | \mathbf{x}_t, \xi_i)\}_{m=1, \dots, M}^{i=1, \dots, d}$ in Eq. (4)

7: **for** $i = 1, \dots, d$ **do**

8: Compute $\tilde{\mathcal{G}}^M[G_{\sigma_i}(0 | \mathbf{x}_t, \xi_i)]$ in Eq. (9)

9: **end for**

10: Assemble $\tilde{\nabla}_{\sigma, \Xi}^M[F](\mathbf{x}_t)$ in Eq. (11)

11: Set $\mathbf{x}_{t+1} = \mathbf{x}_t - \lambda \tilde{\nabla}_{\sigma, \Xi}^M[F](\mathbf{x}_t)$

12: **if** $\|\tilde{\nabla}_{\sigma, \Xi}^M[F](\mathbf{x}_t)\|_2 < \gamma$ **then**

13: Generate $\Delta\Xi$ and update $\Xi = \mathbf{I}_d + \Delta\Xi$

14: Generate σ_i from $U(r - \beta, r + \beta)$ for $i = 1, \dots, d$

15: **end if**

16: **end for**

3.3. Theoretical results

In the following, we verify that the DGS-gradient operator converges to ∇F when $\sigma \rightarrow 0$, and based on that, establish the convergence rate for the method in local regime. Even though our primary focus is not to employ DGS-gradient operator as a conventional gradient estimator, we show that when used for that purpose, this operator is also very competitive and can provide accurate gradient estimate under a weak condition.

In this section, we assume F is convex and differentiable. We say $F \in C^{1,1}(\mathbb{R}^d)$ if there exists $L_1(F) > 0$ such that

$$\|\nabla F(\mathbf{x} + \xi) - \nabla F(\mathbf{x})\| \leq L_1(F)\|\xi\|, \forall \mathbf{x}, \xi \in \mathbb{R}^d.$$

For ξ being a unit vector in \mathbb{R}^d , we define $\nabla_{\xi} F(\mathbf{x})$ the partial derivatives of F at $\mathbf{x} \in \mathbb{R}^d$ in direction ξ , i.e.,

$$\nabla_{\xi} F(\mathbf{x}) = \langle \nabla F(\mathbf{x}), \xi \rangle.$$

We say $F \in C^{1,1}(\mathbb{R}^d)$ is a strongly convex function if there exists a positive number τ such that for any $\mathbf{x}, \xi \in \mathbb{R}^d$,

$$F(\mathbf{x} + \xi) \geq F(\mathbf{x}) + \langle \nabla F(\mathbf{x}), \xi \rangle + \frac{\tau}{2}\|\xi\|^2.$$

We will refer to τ as the *convexity parameter* of F .

First, adapting Lemma 3, (Nesterov & Spokoiny, 2015) to 1-dimensional Gaussian smoothing, we arrive at the following bounds on partial derivative estimates.

Lemma 1. Let ξ be a unit vector in \mathbb{R}^d and F be a function in $C^{1,1}(\mathbb{R}^d)$. For $\mathbf{x} \in \mathbb{R}^d$, define $G_{\sigma}(\cdot | \mathbf{x}, \xi)$ as in (5). There hold

$$i) |\mathcal{D}[G_{\sigma}(0 | \mathbf{x}, \xi)] - \nabla_{\xi} F(\mathbf{x})| \leq 4\sigma L_1(F), \quad (13)$$

$$ii) |\mathcal{D}[G_{\sigma}(0 | \mathbf{x}, \xi)]| \leq 4\sigma L_1(F) + |\nabla_{\xi} F(\mathbf{x})|. \quad (14)$$

These results give us the gradient estimates using DGS-gradient operator.

Lemma 2. Let $\Xi = \{\xi_1, \dots, \xi_d\}$ be a set of orthonormal vectors in \mathbb{R}^d and F be a function in $C^{1,1}(\mathbb{R}^d)$, $\forall 1 \leq i \leq d$. Then

$$i) \|\tilde{\nabla}_{\sigma, \Xi}^M[F](\mathbf{x}) - \nabla F(\mathbf{x})\|^2 \quad (15)$$

$$\leq \frac{2C_0^2\pi(M!)^2}{4^M((2M)!)^2} \sum_{i=1}^d \sigma_i^{4M-2} + 32L_1^2(F) \sum_{i=1}^d \sigma_i^2,$$

$$ii) \|\tilde{\nabla}_{\sigma, \Xi}^M[F](\mathbf{x})\|^2 \leq 64L_1^2(F) \sum_{i=1}^d \sigma_i^2 \quad (16)$$

$$+ 4 \sum_{i=1}^d |\nabla_{\xi_i} F(\mathbf{x})|^2 + \frac{2C_0^2\pi(M!)^2}{4^M((2M)!)^2} \sum_{i=1}^d \sigma_i^{4M-2}.$$

Proof. From (10) and (13), we have for any $i \in \{1, \dots, d\}$

$$\left| \tilde{\mathcal{G}}^M[G_{\sigma_i}(0 | \mathbf{x}, \xi_i)] - \nabla_{\xi_i} F(\mathbf{x}) \right|^2 \quad (17)$$

$$\leq 2 \left| \tilde{\mathcal{G}}^M[G_{\sigma_i}] - \mathcal{D}[G_{\sigma_i}] \right|^2 + 2 \left| \mathcal{D}[G_{\sigma_i}] - \nabla_{\xi_i} F(\mathbf{x}) \right|^2$$

$$\leq \frac{2C_0^2(M!)^2\pi}{4^M((2M)!)^2} \sigma_i^{4M-2} + 32\sigma_i^2 L_1^2(F)$$

Summing (17) from $i = 1$ to d gives (15). For (16), recall

$$\|\tilde{\nabla}_{\sigma, \Xi}^M[F](\mathbf{x})\|^2 = \sum_{i=1}^d \left| \tilde{\mathcal{G}}^M[G_{\sigma_i}(0 | \mathbf{x}, \xi_i)] \right|^2. \quad (18)$$

Each term inside the above sum can be bounded as

$$\begin{aligned} \left| \tilde{\mathcal{G}}^M[G_{\sigma_i}(0 | \mathbf{x}, \xi_i)] \right|^2 &\leq 2 \left| \mathcal{D}[G_{\sigma_i}(0 | \mathbf{x}, \xi_i)] \right|^2 \\ &+ 2 \left| \tilde{\mathcal{G}}^M[G_{\sigma_i}(0 | \mathbf{x}, \xi_i)] - \mathcal{D}[G_{\sigma_i}(0 | \mathbf{x}, \xi_i)] \right|^2 \\ &\stackrel{(10),(14)}{\leq} 64\sigma_i^2 L_1^2(F) + 4|\nabla_{\xi_i} F(\mathbf{x})|^2 + \frac{2C_0^2(M!)^2\pi}{4^M((2M)!)^2} \sigma_i^{4M-2}. \end{aligned}$$

Plugging this into (18), we obtain (16). \square

Assume that we apply the smoothing parameter $\sigma_i = \sigma$ for every direction, from (15), the condition under which DSG-ES ensures $\|\tilde{\nabla}_{\sigma, \Xi}^M[F](\mathbf{x}) - \nabla F(\mathbf{x})\| \leq \varepsilon$ is

$$\sigma \leq \frac{\varepsilon}{4L_1(F)\sqrt{d}}, \# \text{ of samples} = dM \geq d \log \left(\frac{2d}{\varepsilon^2} \right)$$

Compared to other methods of gradient approximations (Behrahas et al., 2019b), our condition on σ is comparable to Forward Finite Difference and Sphere Smoothed (Flaxman et al., 2005) up to a constant, and superior to Gaussian Smoothed (Salimans et al., 2017), which is $\sigma \leq \frac{\varepsilon}{L_1 d}$. The number of function evaluations required is slightly more demanding than those of Forward and Central Finite Difference, which are $d+1$ and $2d$ respectively, but in general better than Gaussian Smoothed and Sphere Smoothed, which are $O(\frac{d}{\varepsilon^2})$ and $O(\frac{d}{\varepsilon^2} \log(d))$ respectively.

With the gradient estimate (15), we will be able to establish error estimates for DGS-ES. We show here a convergence rate of our method in optimizing strongly convex functions.

Theorem 1 (DGS-ES for strongly convex function). *Let F be a strongly convex function in $C^{1,1}(\mathbb{R}^d)$ and the sequence $\{\mathbf{x}_t\}_{t \geq 0}$ be generated by Algorithm 1 with $\lambda = \frac{1}{8L_1(F)}$.*

Then, for any $t \geq 0$, we have

$$F(\mathbf{x}_t) - F(\mathbf{x}^*) \leq \frac{1}{2}L_1(F) \left[\delta_\sigma + \left(1 - \frac{\tau}{16L_1(F)}\right)^t (\|\mathbf{x}_0 - \mathbf{x}^*\|^2 - \delta_\sigma) \right]. \quad (19)$$

Here,

$$\delta_\sigma = \left(\frac{128}{\tau^2} + \frac{16}{\tau L_1(F)} \right) L_1^2(F) \sum_{i=1}^d \sigma_i^2 + \left(\frac{8}{\tau^2} + \frac{1}{2\tau L_1(F)} \right) \frac{C_0^2(M!)^2 \pi}{4^M((2M)!)^2} \sum_{i=1}^d \sigma_i^2, \quad (20)$$

where τ, σ are the convexity and smoothing parameters and M is the number of Gauss-Hermite samples.

Proof. Denote $r_t = \|\mathbf{x}_t - \mathbf{x}^*\|$, where \mathbf{x}^* is the global minimizer of F . Then

$$\begin{aligned} r_{t+1}^2 &= \|\mathbf{x}_t - \lambda \tilde{\nabla}_{\sigma, \Xi}^M[F](\mathbf{x}_t) - \mathbf{x}^*\|^2 \quad (21) \\ &= r_t^2 - 2\lambda \langle \tilde{\nabla}_{\sigma, \Xi}^M[F](\mathbf{x}_t), \mathbf{x}_t - \mathbf{x}^* \rangle + \lambda^2 \|\tilde{\nabla}_{\sigma, \Xi}^M[F](\mathbf{x}_t)\|^2 \\ &\stackrel{(16)}{=} r_t^2 - 2\lambda \langle \tilde{\nabla}_{\sigma, \Xi}^M[F](\mathbf{x}_t) - \nabla F(\mathbf{x}_t), \mathbf{x}_t - \mathbf{x}^* \rangle \\ &\quad - 2\lambda \langle \nabla F(\mathbf{x}_t), \mathbf{x}_t - \mathbf{x}^* \rangle + 4\lambda^2 \sum_{i=1}^d |\nabla_{\xi_i} F(\mathbf{x}_t)|^2 \\ &\quad + 64\lambda^2 L_1^2(F) \sum_{i=1}^d \sigma_i^2 + \frac{2C_0^2 \lambda^2 (M!)^2 \pi}{4^M((2M)!)^2} \sum_{i=1}^d \sigma_i^{4M-2}. \end{aligned}$$

We proceed to bound the right hand side of (21). First, since F is strongly convex,

$$\begin{aligned} -2\lambda \langle \nabla F(\mathbf{x}_t), \mathbf{x}_t - \mathbf{x}^* \rangle &\leq 2\lambda F(\mathbf{x}^*) \\ -2\lambda F(\mathbf{x}_t) - \lambda\tau \|\mathbf{x}^* - \mathbf{x}_t\|^2 &\leq 0. \end{aligned} \quad (22)$$

On the other hand,

$$\begin{aligned} -2\lambda \langle \tilde{\nabla}_{\sigma, \Xi}^M[F](\mathbf{x}_t) - \nabla F(\mathbf{x}_t), \mathbf{x}_t - \mathbf{x}^* \rangle &\leq \frac{2\lambda}{\tau} \|\tilde{\nabla}_{\sigma, \Xi}^M[F](\mathbf{x}_t) - \nabla F(\mathbf{x}_t)\|^2 + \frac{\lambda\tau}{2} \|\mathbf{x}_t - \mathbf{x}^*\|^2 \quad (23) \\ &\stackrel{(15)}{\leq} \frac{4\lambda}{\tau} \cdot \frac{C_0^2 \pi (M!)^2}{4^M((2M)!)^2} \sum_{i=1}^d \sigma_i^{4M-2} \\ &\quad + \frac{64\lambda}{\tau} L_1^2(F) \sum_{i=1}^d \sigma_i^2 + \frac{\lambda\tau}{2} \|\mathbf{x}_t - \mathbf{x}^*\|^2. \end{aligned}$$

Applying an estimate for convex, $C^{1,1}$ -functions, see, e.g., Theorem 2.1.5, (Nesterov, 2004), gives

$$\begin{aligned} 4\lambda^2 \sum_{i=1}^d |\nabla_{\xi_i} F(\mathbf{x}_t)|^2 &= 4\lambda^2 \|\nabla F(\mathbf{x}_t)\|^2 \quad (24) \\ &\leq 8\lambda^2 L_1(F) (F(\mathbf{x}_t) - F(\mathbf{x}^*)). \end{aligned}$$

Combining (21)–(24), there holds

$$\begin{aligned} r_{t+1}^2 &\leq r_t^2 - (2\lambda - 8\lambda^2 L_1(F)) (F(\mathbf{x}_t) - F(\mathbf{x}^*)) \\ &\quad + \left(\frac{64\lambda}{\tau} + 64\lambda^2 \right) L_1^2(F) \sum_{i=1}^d \sigma_i^2 \quad (25) \\ &\quad + \left(\frac{4\lambda}{\tau} + 2\lambda^2 \right) \frac{C_0^2 (M!)^2 \pi}{4^M((2M)!)^2} \sum_{i=1}^d \sigma_i^{4M-2}. \end{aligned}$$

Since F is a strongly convex function, for $\lambda = 1/(8L_1(F))$ we have that

$$\begin{aligned} - (2\lambda - 8\lambda^2 L_1(F)) (F(\mathbf{x}_t) - F(\mathbf{x}^*)) \\ \leq \frac{\tau}{16L_1(F)} \|\mathbf{x}_t - \mathbf{x}^*\|^2. \end{aligned} \quad (26)$$

Assuming $\sigma_i < 1, \forall i$. We derive from (25), (26) and (20) that $r_{t+1}^2 - \delta_\sigma \leq \left(1 - \frac{\tau}{16L_1(F)}\right) (r_t^2 - \delta_\sigma)$, which yields

$$r_t^2 - \delta_\sigma \leq \left(1 - \frac{\tau}{16L_1(F)}\right)^t (r_0^2 - \delta_\sigma).$$

Note that $F(\mathbf{x}_t) - F(\mathbf{x}^*) \leq \frac{1}{2}L_1(F) \|\mathbf{x}_t - \mathbf{x}^*\|^2$, since $f \in C^{1,1}(\mathbb{R}^d)$, we arrive at the conclusion. \square

It is worth remarking a few things on the above theorem. First, we obtain the global linear rate of convergence with DGS-ES, which is expected for strongly convex functions.

Second, the result allows certain random perturbation of Ξ and σ . In particular, Theorem 1 still holds with Ξ and σ changing after each iterate, as long as Ξ remains orthonormal and $\|\sigma\|$ is fixed.

Let us conclude this section by comparing conditions that guarantee $F(\mathbf{x}_t) - F(\mathbf{x}^*) \leq \varepsilon$ of our method with that of random search GS approach in (Nesterov & Spokoiny, 2015) in this strongly convex setting. Assume again $\sigma_i = \sigma$ for every direction. From error estimate (19), we need to choose

$$\sigma \leq O\left(\sqrt{\frac{\varepsilon}{d}}\right), \# \text{ of samples} = dM \geq O\left(d \log\left(\frac{d}{\varepsilon}\right)\right),$$

$$\# \text{ of iterations} = O\left(\log\frac{1}{\varepsilon}\right).$$

The corresponding condition for random search GS is

$$\sigma \leq O\left(\sqrt{\frac{\varepsilon}{d}}\right), \# \text{ of samples} = \# \text{ of iter.} = O\left(d \log\frac{1}{\varepsilon}\right).$$

The number of iterates in (Nesterov & Spokoiny, 2015) scales linearly with the dimension, which is undesirable for high-dimensional problems. This method however evaluates only one sample per iterate, thus, the total number of function evaluations remains low. Our method requires a slightly higher number of samples. However, it is possible to parallelize the function evaluations over thousands of workers at each step, so our number of iteration is completely independent of dimension. This makes DGS-ES very well-suited for large distributed computer systems.

4. Experiments

We evaluate the proposed DGS-ES method using three sets of problems, i.e., benchmark functions in low and medium dimensions (2D to 10D), benchmark functions in very high-dimensional spaces (1000D and 2000D), and a real-world aerospace structure design problem. We compared the DGS-ES method with the following blackbox optimization methods: (a) Evolution Strategy (ES) in (Salimans et al., 2017); (b) Covariance matrix adaptation evolution strategy (CMA-ES) in (Hansen, 2006) (we used the implementation of CMA-ES in the pycma open-source code from <https://github.com/CMA-ES/pycma>), (c) Trust-Region Bayesian Optimization (TuRBO) in (Eriksson et al., 2019) (we used the code released by the authors at <https://github.com/uber-research/TuRBO>) and (d) the BFGS method.

4.1. Tests on functions in low to medium dimension

We tested our method and the baselines in nine benchmark problems (Surjanovic & Bingham), including 2D-Ackley (Ackley2), 5D-Ackley (Ackley5), 10D-Ackley (Ackley10),

2D-Branin (Branin), 10D-Levy (Levy10), 2D-Cross-In-Tray (CrossInTray), 10D-Sphere (Sphere10), 2D-DropWare (Dropwave) and 10D-Rastrigin (Rastrigin10). In our tests, we used the same parameter and input domains as in (Surjanovic & Bingham).

For each benchmark function, we performed 20 repeated independent trials for each method to show the statistical performance. Three metrics are used to compare the performance of our method and the baselines:

- Success rate, i.e., the percentage of successful convergence to the global minimum of each test function.
- The average iterations needed for global convergence, which only takes into account the successful trials.
- The averaged minimal objective function value found in the unsuccessful trials.

The comparison results for the three metrics are given in Table 1, Table 2, Table 3, respectively.

Table 1 shows that both the DGS-ES and the baselines perform perfectly for Sphere10 (a convex function), and Branin (a low-dimensional near convex function). For non-convex functions, our method performs better than the other baselines when the function has global funnel type structures, i.e., the Ackley functions, Levy10, Dropwave, and Rastrigin10. This is due to the nonlocal exploitation ability of the DGS-ES method when using with relatively large standard deviations σ , e.g., $\sigma = 1.0$. However, when a function does not have an obvious funnel shape, e.g., the CrossIn-Tray function, the success rate of the DGS-ES method drops dramatically, regardless of the dimension.

Table 2 indicates the convergence speed of an optimization method in a successful trial. When a method has 0% success rate in Table 1, “ ∞ ” is placed in the corresponding spots in Table 2. We observed that the DGS-ES and the ES methods need the most iterations to achieve global convergence, because no adaptive strategies, e.g., adaptive learning rate, is used to accelerate the convergence. The BFGS method converges very fast when it can find the global minima. Both CMA-ES and TuRBO methods have some kind of adaptive strategy, e.g., adjusting covariance matrix in CMA-ES or the trust region radius in TuRBO, to help achieve faster convergence. However, if the adaptive adjustment is based on incorrect information, those methods may fail to converge, which could be the reason why their success rates are lower than the DGS-ES method for most test functions.

Table 3 indicates what kind of local minima an algorithm is trapped in a unsuccessful trial. We can see that DGS-ES performs better than the baselines in most cases, due to its nonlocal exploitation capability. For further illustration, we plotted in Figure 2 the DGS-gradient direction and local gradient direction at 50 random locations on the surface of the Ackley2. The standard deviation σ used in directional

Gaussian smoothing is set to 0.01 in Figure 2(Left) and 1.0 in Figure 2(Right). It shows that the DGS-gradient with larger σ mostly points to the global minimum at $(0, 0)$.

Table 1. Comparison between the DGS-ES method and the baselines on Metric (a) the success rate, i.e., the percentage of successful convergence to the global minimum.

	DGS-ES	ES	CMA-ES	TuRBO	BFGS
Ackley2	95%	75%	65%	100%	0%
Ackley5	90%	85%	50%	55%	0%
Ackley10	90%	85%	45%	45%	0%
Branin	100%	100%	100%	100%	100%
Levy10	100%	50%	55%	15%	0%
CrossInTray	60%	5%	30%	65%	10%
Sphere10	100%	100%	100%	100%	100%
Dropwave	100%	100%	55%	100%	10%
Rastrigin10	100%	85%	0%	0%	0%

Table 2. Comparison between the DGS-ES method and the baselines on Metric (b) the average iterations needed for global convergence, which only takes into account the successful trials.

	DGS-ES	ES	CMA-ES	TuRBO	BFGS
Ackley2	774	829	38	513	∞
Ackley5	1014	1894	59	1278	∞
Ackley10	2603	4321	160	3980	∞
Branin	205	160	17	152	4
Levy10	2215	16331	70	706	∞
CrossInTray	2901	4265	38	490	3
Sphere10	206	996	47	30	3
Dropwave	720	1765	16	458	2
Rastrigin10	1406	7347	∞	∞	∞

Table 3. Comparison between the DGS-ES method and other methods on Metric (c) the averaged minimal objective function value found in the unsuccessful trials. The global minima of the test functions are: Ackley $F^* = 0$, Branin $F^* = 0.399$, Levy10 $F^* = 0$, CrossInTray $F^* = -2.062$, Sphere10 $F^* = 0$, Dropwave $F^* = -1$, Rastrigin $F^* = 0$.

	DGS-ES	ES	CMA-ES	TuRBO	BFGS
Ackley2	6.08	20.33	16.53	-	17.36
Ackley5	18.84	20.62	14.06	2.75	19.32
Ackley10	5.52	19.68	19.01	9.57	19.24
Branin	-	-	-	-	-
Levy10	-	4.96	6.45	7.59	18.78
CrossInTray	-0.995	1.05	2.31	3.49	1.93
Sphere10	-	-	-	-	-
Dropwave	-	-	1.13	-	2.46
Rastrigin10	-	7.98	16.85	21.39	86.31

4.2. Tests on high-dimensional functions

Here we investigate the DGS-ES performance on the high-dimensional functions: Sphere, Ackley (Re-scaled), Levy

and Rastrigin functions, in 100D, 1000D and 2000D. The original Ackley function is extremely difficult in high dimensions, because its Lipschitz constant does not grow with the dimension and it is a highly concave function. In order to use the Ackley-type of geometry to test our DGS-ES method, we enlarged its Lipschitz constant by multiplying the original Ackley function by 100, and reducing the search domain to $[-10.0, 10.0]^d$.

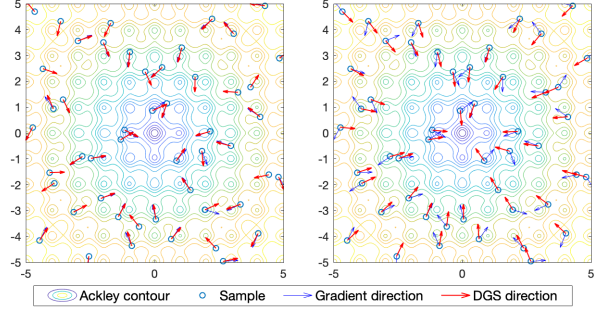


Figure 2. Illustration of DGS-gradient direction and local gradient direction at 50 random locations on the surface of the Ackley2. (Left) The standard deviation σ is set to 0.01, such that the DGS-gradient align with the local gradient at most locations. (Right) The standard deviation σ is set to 1.0, such that most DGS-gradient points to the global minimum at $(0, 0)$.

Figure 3 shows the scalability of the DGS-ES algorithm with the dimension of the objective function. We performed 20 repeated independent trials for each method to show the sta-

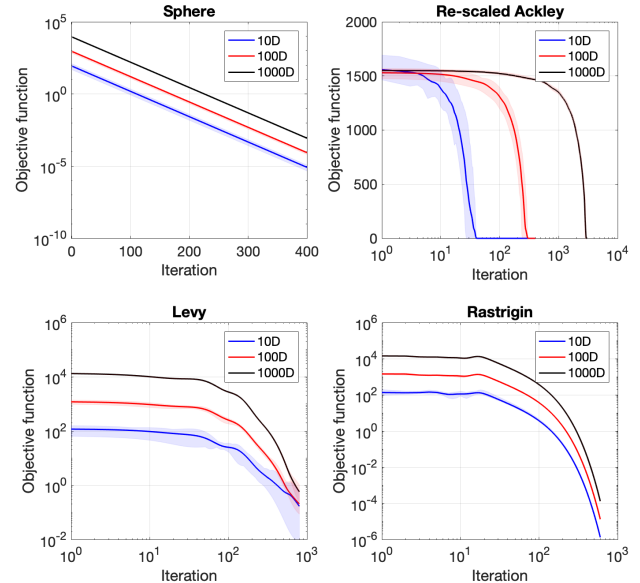


Figure 3. Illustration of the dimension dependence of the convergence rate of the DGS-ES method. The convergence rate, i.e., the number of iterations to converge, is independent of the dimension for convex functions, e.g., Sphere function, which is consistent with our theoretical analysis in §3.3.

tistical performance. In §3.3, we proved in Theorem 1 that the DGS-ES method can achieve dimension independent convergence rate when optimizing strongly convex functions. Our numerical results are consistent with Theorem 1. For example, for the sphere function, the convergence rate does not change when we increase the dimension from 10 to 1000. Moreover, such property carries over to the non-convex Levy and Rastrigin. The reason is that both Levy and Rastrigin have a globally near-convex structure when smoothing out their local minima. In contrast, the Ackley function is highly concave, as a large part of its surface is almost flat regardless of the small local minima. In this case, it takes many iterations for DGS-ES to search for the global minimum hidden in the middle of the flat surface.

Figure 4 shows the comparison between the DGS-ES and the baselines for optimizing the four benchmark functions in Figure 3 in 2000-dimensional space. For the sphere function, BFGS is a clear winner due to its optimal performance in handling convex functions. Among the three ES-type methods, the DGS-ES has much better performance than its competitors. For the other three functions, the DGS-ES method shows significant advantages over other methods.

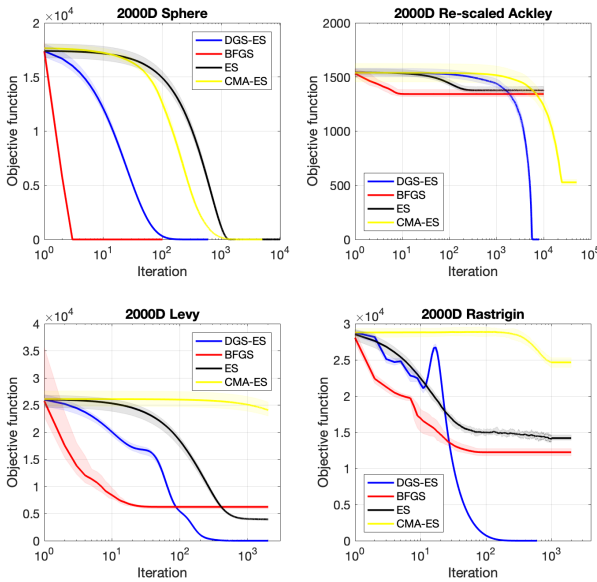


Figure 4. Comparison of different blackbox optimization methods on four 2000-dimensional benchmark functions.

4.3. Aerospace hierarchical stiffened shell design

Now we demonstrate the DGS-ES method on a real-world stiffened shell design problem. Due to its high strength and stiffness, the hierarchical stiffened shell has been widely used in aerospace engineering. However, it is challenging to fully explore its optimal buckling load-carrying capacity. The goal of this work is to improve the load-carrying capacity by optimizing the representative unit cell of hierarchical

stiffened shell where the inputs are 9 size variables (widths, heights and thickness) for major and minor stiffeners, as shown in Figure 5(a), and the output is the carrying-load capability factor which is calculated by high-fidelity numerical simulation, e.g. finite element method (FEM), see Figure 5 (b). Although the high-fidelity FEM simulation is time-consuming, many open-source codes and commercial software have improved the computational efficiency via scalable parallelism and GPU acceleration. It is thus feasible to apply the DGS-ES method by implementing parallel FEM simulations in supercomputers. Figure 5 presents the comparison between DGS-ES and the other blackbox optimization methods. We observed that DGS-ES outperforms all other algorithms and achieves faster convergence using only 100 iterations. The robustness of DGS-ES also outperforms the alternatives.

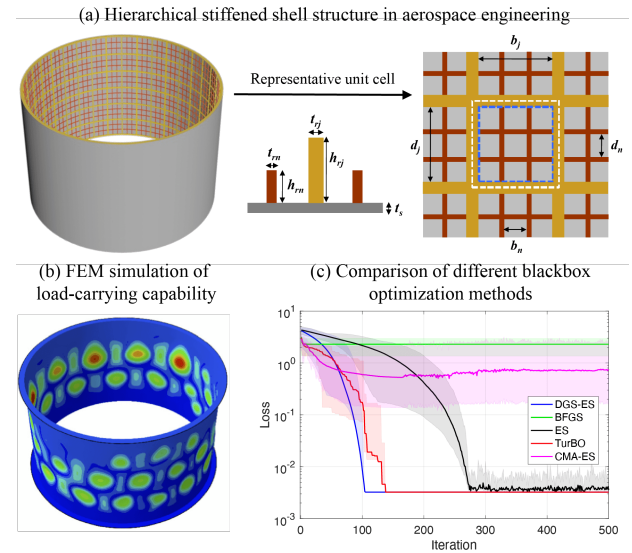


Figure 5. Illustration and design optimization of hierarchical stiffened shell structures in aerospace engineering, e.g. rocket.

5. Discussion on the limitations of DGS-ES

Despite the successful demonstration of the DGS-ES method shown in §4, we realized that there are several limitations with the current version of the DGS-ES algorithm, including: (a) *Naive random perturbation strategy for exploration.* As the estimator $\tilde{\nabla}_{\sigma, \Xi}^M[F]$ is deterministic, an effective random exploration strategy is critically important to the robustness of the algorithm. The current random rotation algorithm does not effectively exploit the $d(d-1)/2$ degrees of freedom of the special orthogonal group $SO(d)$, such that important information may be lost after the perturbation. (b) *The need for hyper-parameter tuning.* The most sensitive hyper-parameter is standard deviation σ in $\tilde{\nabla}_{\sigma, \Xi}^M[F]$. If σ is too small, the function is insufficiently smoothed, such that the optimizer may be trapped in a local minimum. In contrast, if σ is too big, the function is over

smoothed, such that the convergence will become much slower. An adaptive strategy, e.g., the covariance matrix adaptation in CMA-ES, will be needed to alleviate such issue.

Acknowledgement

This material was based upon work supported by the U.S. Department of Energy, Office of Science, Office of Advanced Scientific Computing Research, Applied Mathematics program under contract and award numbers ERKJ352, and by the Artificial Intelligence Initiative at the Oak Ridge National Laboratory (ORNL). ORNL is operated by UT-Battelle, LLC., for the U.S. Department of Energy under Contract DE-AC05-00OR22725.

References

- Abramowitz, M. and Stegun, I. (eds.). *Handbook of Mathematical Functions*. Dover, New York, 1972.
- Berahas, A. S., Cao, L., Choromanski, K., and Scheinberg, K. Linear interpolation gives better gradients than gaussian smoothing in derivative-free optimization. *arXiv preprint arXiv:1905.13043*, 2019a.
- Berahas, A. S., Cao, L., Choromanski, K., and Scheinberg, K. A theoretical and empirical comparison of gradient approximations in derivative-free optimization. *arXiv:1905.01332*, 2019b.
- Choromanski, K., Rowland, M., Sindhvani, V., Turner, R. E., and Weller, A. Structured evolution with compact architectures for scalable policy optimization. *International Conference on Machine Learning*, pp. 969–977, 2018.
- Choromanski, K., Pacchiano, A., Parker-Holder, J., , and Tang, Y. From complexity to simplicity: Adaptive esactive subspaces for blackbox optimization. *NeurIPS 2019*, 2019a.
- Choromanski, K., Pacchiano, A., Parker-Holder, J., , and Tang, Y. Provably robust blackbox optimization for reinforcement learning. *arXiv:1903.02993*, 2019b.
- Cui, X., Zhang, W., Tüske, Z., and Picheny, M. Evolutionary stochastic gradient descent for optimization of deep neural networks. *NeurIPS*, 2018.
- Eriksson, D., Pearce, M., Gardner, J., Turner, R. D., and Poloczek, M. Scalable global optimization via local bayesian optimization. In *Advances in Neural Information Processing Systems*, pp. 5497–5508, 2019.
- Fazel, M., Ge, R., Kakade, S. M., and Mesbahi, M. Global convergence of policy gradient methods for the linear quadratic regulator. *Proceedings of the 35th International Conference on Machine Learning*, 80:1467–01476, 2018.
- Flaxman, A. D., Kalai, A. T., Kalai, A. T., and McMahan, H. B. Online convex optimization in the bandit setting: gradient descent without a gradient. *Proceedings of the 16th Annual ACM-SIAM symposium on Discrete Algorithms*, pp. 385–394, 2005.
- Ha, D. and Schmidhuber, J. Recurrent world models facilitate policy evolution. *Advances in Neural Information Processing Systems*, pp. 2450–2462, 2018.
- Hansen, N. The cma evolution strategy: a comparing review. In *Towards a new evolutionary computation*, pp. 75–102. Springer, 2006.
- Hansen, N. The cma evolution strategy: A tutorial. *arXiv preprint arXiv:1604.00772*, 2016.
- Hansen, N. and Ostermeier, A. Completely derandomized self-adaptation in evolution strategies. *Evolutionary computation*, 9(2):159–195, 2001.
- Houthoofd, R., Chen, Y., Isola, P., Stadie, B., Wolski, F., Ho, O. J., and Abbeel, P. Evolved policy gradients. *Advances in Neural Information Processing Systems*, pp. 5400–5409, 2018.
- Larson, J., Menickelly, M., and Wild, S. M. Derivative-free optimization methods. *Acta Numerica*, 28:287–404, 2019.
- Maggiar, A., Wachter, A., Dolinskaya, I. S., and Staum, J. A derivative-free trust-region algorithm for the optimization of functions smoothed via gaussian convolution using adaptive multiple importance sampling. *SIAM Journal on Optimization*, 28(2):1478–1507, 2018.
- Maheswaranathan, N., Metz, L., Tucker, G., Choi, D., and Sohl-Dickstein, J. Guided evolutionary strategies: Augmenting random search with surrogate gradients. *Proceedings of the 36th International Conference on Machine Learning*, 2019.
- Meier, F., Mujika, A., Gauy, M. M., and Steger, A. Improving gradient estimation in evolutionary strategies with past descent directions. *Optimization Foundations for Reinforcement Learning Workshop at NeurIPS 2019*, 2019.
- Metz, L., Maheswaranathan, N., Nixon, J., Freeman, D., and Sohl-dickstein, J. Learned optimizers that outperform sgd on wall-clock and test loss. *2nd Workshop on Meta-Learning at NeurIPS*, 2018.
- Miikkulainen, R., Liang, J., Meyerson, E., Rawal, A., Fink, D., Francon, O., Raju, B., Shahrzad, H., Navruzyan, A., Nuffy, N., and Hodjat, B. Evolving deep neural networks. *arXiv preprint arXiv:1703.00548*, 2017.

- Morse, G. and Stanley, K. O. Simple evolutionary optimization can rival stochastic gradient descent in neural networks. *Proceedings of the Genetic and Evolutionary Computation Conference (GECCO 2016)*, pp. 477–484, 2016.
- Nesterov, Y. *Introductory Lectures on Convex Optimization*. Springer US, 2004.
- Nesterov, Y. and Spokoiny, V. Random gradient-free minimization of convex functions. *Foundations of Computational Mathematics*, pp. 1–40, 2015.
- Quarteroni, A., Sacco, R., and Saleri, F. *Numerical Mathematics*, volume 332. Springer Science Business Media &, 2007.
- Real, E., Moore, S., Selle, A., Saxena, S., Suematsu, Y. L., Tan, J., Le, Q. V., and Kurakin, A. Large-scale evolution of image classifiers. *International Conference on Machine Learning (ICML)*, pp. 2902–2911, 2017.
- Rechenberg, I. and Eigen, M. *Evolutionsstrategie: Optimierung Technischer Systeme nach Prinzipien der Biologischen Evolution*. Frommann-Holzboog Stuttgart, 1973.
- Rios, L. M. and Sahinidis, N. V. Derivative-free optimization: a review of algorithms and comparison of software implementations. *J Glob Optim*, 56:1247–1293, 2009.
- Salimans, T., Ho, J., Chen, X., and Sutskever, I. Evolution strategies as a scalable alternative to reinforcement learning. *arXiv preprint arXiv:1703.03864*, 2017.
- Schwefel, H.-P. *Numerische optimierung von computermodellen mittels der evolutionsstrategie*. 1977.
- Surjanovic, S. and Bingham, D. Virtual library of simulation experiments: Test functions and datasets. Retrieved February 6, 2020, from <http://www.sfu.ca/~ssurjano>.
- Wierstra, D., Schaul, T., Glasmachers, T., Sun, Y., Peters, J., and Schmidhuber, J. Natural evolution strategies. *Journal of Machine Learning Research*, 15:949–980, 2014.